Chalcogenide Letters Vol. 12, No. 11, November 2015, p. 597 - 607

DEDUCTION OF THE LUMINESCENCE PARAMETERS OF TELLURIUM OXIDE BASED GLASSES DOPED WITH Er^{3+} IONS

E. S. YOUSEF[ab*], M. M. ELOKR[b], Y. M. ABOUDEIF[b]
[a]*Physics Department, Faculty of Science, Al- Azhar University, Assiut branch, Assiut, Egypt.*
[b]*Physics Department, Faculty of Science, Al-Azhar University, Naser city 11884, Cairo, Egypt.*

Quaternary glasses within system $75TeO_2$-$10Nb_2O_5$-10ZnO- 5PbO doped with different concentration of Er_2O_3 ions were prepared. The Judd–Ofelt parameters Ω_2, Ω_4, Ω_6, the oscillator strength type transition probabilities, spectroscopic quality factors, branching ratio and radiative lifetimes of several excited states of Er^{3+} have been evaluated. The gain cross-section of laser transition level from $^4I_{13/2} \rightarrow {}^4I_{15/2}$ was obtained. $75TeO_2$-$10Nb_2O_5$-5PbO-10ZnO-8750 ppm Er_2O_3 has the highest effective emission cross section bandwidth (66.3nm) and large stimulated emission cross-section equal 27.96×10^{-21} cm^2. Spectroscopic properties indicate that this glass doped with Er^{3+} is a promising candidate for optical applications.

Received August 23, 2015; Accepted November 13, 2015)

Keywords: Oxide glasses; UV- Vis- NIR; luminescence parameters.

1. Introduction

Recently the development of new materials of TeO_2- based glasses which combine rare earth with are very attractive materials of optical amplifiers in wide range for the wavelength division multiplexing (WDM) network systems [1- 3]. Why TeO_2 based glasses attract more attention; because it have some advantageous properties such as relatively low phonon energy, high refractive index, high dielectric constant, good corrosion resistance, good thermal and chemical stability and low melting point [3]. Moreover in comparison Er^{3+} doped tellurite glasses with halide and sulfides glasses, they have a large emission cross section ($\sigma_e \geq 7.5 \times10^{-21}$ cm^{-2}) and a broad fluorescence band at around 1.55 μm with full width at half maximum (FWHM) of around ≈ 80 nm. Also the TeO_2-based glasses contain the lead oxide are highly polarizable due to the presence of $6S^2$ electrons. These glasses possess a large non-linear optical properties hence they are suitable for potential applications in non-linear optical devices such as broad band optical amplifiers, power limiters and ultra fast switches [4, 5]. It is important to study of the luminescence parameters of the Er^{3+} ions in glass materials such as emission cross-sections, transition probabilities, radiative lifetimes, branching ratios, line widths for the excited states. This data require in design optical devices such as fiber amplifiers, color displays and light emitting diodes (LEDs). Besides that the stimulated emission cross- section, fluorescence life-time and optical efficiency are the important properties required for a laser medium are high gain, high energy storage capability and low optical losses [6- 13]. We incorporation heavy metal oxide (HMO) glasses like that PbO and Nb_2O_5 to find their importance as host matrices for good lasing candidates because of their low phonon energy, high thermal stability, high cross-section emission and good solubility of rare earth ions. We used Judd–Ofelt theory [8, 9] to estimated

*Corresponding author: omn_yousef2000@yahoo.com

ratios (β_R) and radiative lifetimes (τ_R) were determined for the excitation level $^4I_{15/2}$. Motivated by concerning these works, tellurium- niobium- lead- zinc oxide glasses doped with Er^{3+} ions have been prepared and the luminescence properties were studied. The suitability of the samples prepared can be used as the candidate material for optical fiber and active medium for solid lasers.

2. Experimental Procedure

The Er^{3+} ions doped glass systems with a composition of $75TeO_2$-$10Nb_2O_5$-5PbO-10ZnO-xEr_2O_3 (where x = 0.00, 2500, 3750, 5000, 6250, 7500 and 8750 ppm) by using the conventional quench-melting method. The raw materials were powdered and put in the platinum crucible and heated in a melting furnace to a temperature of 920 ^oC kept for 45 min; the melt was stirred from time to time The highly viscous melt was cast in a graphite mold. The quenched samples were annealed at 340 °C for 2 h and then cooled inside the furnace down to room temperature. The absorption spectrum of glass was determined at wavelengths in the range from 200 to 2700 nm, using a Shimadzu 3101PC spectrophotometer.

3. Results and discussion

The variation of the refractive index with different of wavelength given by Sellmeier equations [14]:

$$n^2(\lambda) = A + \frac{B}{1-\frac{C}{\lambda^2}} + \frac{D}{1-\frac{E}{\lambda^2}} \tag{1}$$

where n(λ) represents the refractive index at the wavelength of λ and A, B, C, D, E are the constant parameters were obtained by the fitting function of software Origin Pro 8 (this data summarized in Table 1). The Judd–Ofelt (JO) theory is widely used for predicting the possibility of laser action, as well as of optical amplification, through an analysis of the forced electric dipole transitions within the $4f^n$ configuration of rare-earth ions in different isotropic lattices (crystalline and amorphous) [15- 17]. Here in the absorption bands of sample 2 are corresponding to 1534, 980, 800, 654, 544, 524 and 490 nm which denote to the transitions from $^4I_{15/2}$ to $^4I_{13/2}$, $^4I_{11/2}$, $^4I_{9/2}$, $^4F_{9/2}$, $^4S_{3/2}$, $^2H_{11/2}$ and $^4F_{7/2}$, respectively this shown in Fig 1. Also the peak positions of samples from 2 to 7 each transition levels remains unchanged with different Er_2O_3 concentrations from 2500 to 8750 ppm.

Table 1: Sellmeier coefficients of prepared glasses with different concentration Er^{3+} ions in ppm.

Sample code	Glass composition in mol%	Sellmeier Coefficients $n^2(\lambda) = A + B/(1-C/\lambda^2) + D/(1-E/\lambda^2)$				
		A	B	C	D	E
Sample 1	$75TeO_2$-$10Nb_2O_5$-5PbO-10ZnO	3.1917771	1.0368392	0.065723673	25.554721	125.44
Sample 2	$75TeO_2$-$10Nb_2O_5$-5PbO-10ZnO-2500ppm Er_2O_3	3.1373685	1.0821664	0.069160532	22.480447	125.44
Sample 3	$75TeO_2$-$10Nb_2O_5$-5PbO-10ZnO-3750 ppm Er_2O_3	3.1510617	1.0887224	0.06966904	22.126689	125.44
Sample 4	$75TeO_2$-$10Nb_2O_5$-5PbO-10ZnO-5000 ppm Er_2O_3	3.2119902	1.0680939	0.068635713	23.4732	125.44
Sample 5	$75TeO_2$-$10Nb_2O_5$-5PbO-10ZnO-6250 ppm Er_2O_3	3.2482296	1.0646478	0.067844809	24.211444	125.44
Sample 6	$75TeO_2$-$10Nb_2O_5$-5PbO-10ZnO-7500 ppm Er_2O_3	3.2622634	1.0694197	0.068792171	23.727965	125.44
Sample 7	$75TeO_2$-$10Nb_2O_5$-5PbO-10ZnO-8750 ppm Er_2O_3	3.2762347	1.0749772	0.069563394	23.291895	125.44

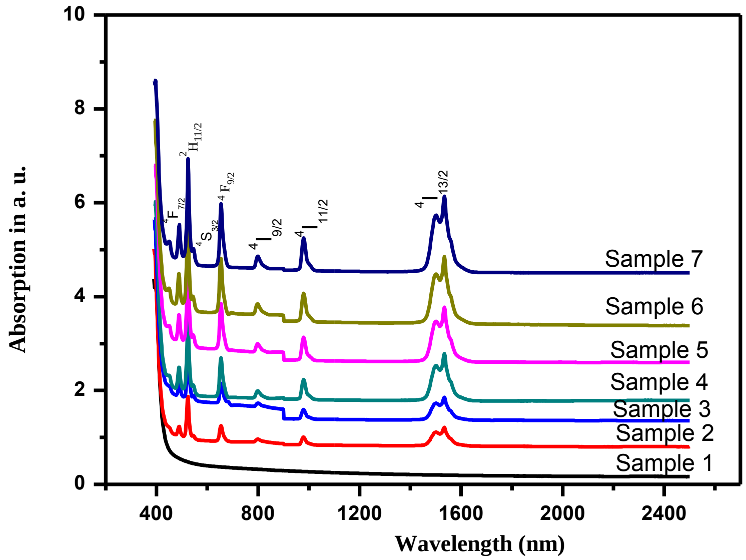

Figure 1: UV–Vis-NIR spectroscopy for prepared glasses.

The measured line strengths, S_{meas} $(J \rightarrow J`)$, of the absorbance band are determined by using the following expression:

$$S_{meas}\ (J \rightarrow J`) = \frac{3ch(2J+1)n}{8\pi^3 \lambda \overline{e^2 N_0}} \left[\frac{9}{(n^2+2)^2}\right] \Gamma \qquad (2)$$

Where J and $J`$ are the total angular momentum quantum numbers of the initial and final states, respectively, n is the refractive index, N_0 is the Er^{3+} ion concentration, λ is the mean wavelength of the specific absorption band, $\Gamma = \int \alpha(\lambda) d\lambda$ is the integrated absorption coefficient as a function of λ, and c and h have their usual meaning. The factor $[9/(n^2+2)^2]$ in Eq. (2) represents the local field correction for the ion in the dielectric host medium [18]. The measured line strengths were then used to obtain the JO parameters Ω_2, Ω_4 and Ω_6 for the corresponding transitions between J and $J`$ manifolds in the following form:

$$S_{calc}(J \rightarrow J') = \sum_{\lambda=2,4,6} \Omega_{(\lambda)} \left|< (S,L)\, J \left\| U^{(\lambda)} \right\| (S',\, L')J' >\right|^2 \qquad (3)$$

Where the matrix elements $\langle \left\| U^{(\lambda)} \right\| \rangle$ are doubly reduced unit tensor operator of the rank, λ, calculated in the intermediate coupling approximation and are independent of the crystal host. However, the parameters Ω_2, Ω_4, and Ω_6 exhibit influence of the host on the transition probabilities since they contain the crystal-field parameters, inter-configurationally radial integrals, and the interaction between the central ion and the intermediate environment. The values of the measured absorption line strengths, S_{meas} are tabulated in Table 2. A least-squares fitting of S_{meas} to S_{calc} provides the following values for the three JO parameters for Er^{3+} in (TNPZ) host material. The Judd–Ofelt intensity parameters $\Omega_{(\lambda)}$ values were calculated by using the $U_{(\lambda)}$ values tabulated by Carnall et al. [19] since they are almost host independent. J–O parameters Ω_{λ} of the $^4I_{13/2}$ metastable level for prepared glasses and some other glasses systems were summarized in Table 3. The highest values of $\Omega_{(\lambda)}$ were obtained for sample 3 (Ω_2 = 3.6005x 10^{-20}

Table 2: Measured and calculated absorption line strengths of Er^{3+} in prepared glasses.

Transition	Wave length (nm)	Energy (cm^{-1})	Sample 2 $S_{(Exp)}$ 10^{-20} cm^2	Sample 2 $S_{(The)}$ 10^{-20} cm^2	Sample 3 $S_{(Exp)}$	Sample 3 $S_{(The)}$	Sample 4 $S_{(Exp)}$	Sample 4 $S_{(The)}$	Sample 5 $S_{(Exp)}$	Sample 5 $S_{(The)}$	Sample 6 $S_{(Exp)}$	Sample 6 $S_{(The)}$	Sample 7 $S_{(Exp)}$	Sample 7 $S_{(The)}$
$^4I_{15/2}\rightarrow{}^4I_{13/2}$	1534	6519	5.4224	6.0378	5.5548	6.7413	3.4052	3.5567	4.8545	5.2872	4.9333	5.2508	4.3856	4.4733
$\rightarrow{}^4I_{11/2}$	980	10204.1	2.5835	1.6596	2.7929	1.7084	1.2816	0.9892	2.1366	1.4220	2.1475	1.4310	1.5986	1.2408
$\rightarrow{}^4I_{9/2}$	800	12500	2.5951	0.4775	4.3637	0.4656	1.0192	0.3044	2.2899	0.3620	2.1303	0.3579	1.2683	0.3332
$\rightarrow{}^4F_{9/2}$	654	15291	3.6881	3.3517	6.1913	5.7950	1.9807	1.8629	3.5561	3.2569	3.2567	2.9360	2.4493	2.2470
$\rightarrow{}^4S_{3/2}$	544	18382.4	1.6977	0.8694	2.1030	0.8977	0.6219	0.5156	1.1462	0.7512	1.0180	0.7569	0.7537	0.6533
$\rightarrow{}^2H_{11/2}$	524	19084	3.8213	4.1921	5.3037	5.9604	2.3918	2.5178	3.2587	3.5948	3.0010	3.3145	2.6196	2.7864
$\rightarrow{}^4F_{7/2}$	490	20408.2	3.1890	2.8848	4.9637	3.6190	1.7211	1.6765	2.7884	2.5914	2.4796	2.5164	1.8933	2.0932
r. m. s. (10^{-20} cm^2)			1.2986		2.3253		0.4070		1.0969		1.0033		0.5312	

Table 3: J- O parameters Ω_λ of the $^4I_{13/2}$ metastable level for prepared glasses

Glasses	Spectroscopic branch Ω_2($x10^{-20}$ cm^2)	Ω_4($x10^{-20}$ cm^2)	Ω_6($x10^{-20}$ cm^2)	Ω_4/Ω_6
Sample 2	3.7126	2.8690	3.9317	0.73
Sample 3	3.6005	7.3223	4.0596	1.804
Sample 4	2.3811	1.4684	2.3316	0.63
Sample 5	2.7793	3.1533	3.3968	0.93
Sample 6	2.7424	2.5315	3.4229	0.74
Sample 7	2.5731	1.6485	2.9545	0.56

We note that the large Ω_2-values are attributed to stronger covalent bonds to the host matrix which increase with increasing Er^{3+} concentration. The quality of the fit is expressed by the magnitude of the root-mean-square deviation (r. m. s.), defined by:

$$\text{r.m.s.} = [\sum_p (S_{calc} - \frac{S_{meas})^2}{p-3}]^{\frac{1}{2}} \qquad (4)$$

Where, p, is the number of observed transitions on the absorption spectrum. The radiative lifetime, τ_R, of the excited state $J`$ is simply related to the total spontaneous emission probability $A_{J`J}$ by:

$$\tau_R = \frac{1}{A_{J`J}} \quad \text{with } A_{J`J} = \sum_{J''} A_{J`J''} \qquad (5)$$

Where, J″, being the intermediate states lying between, J′, and J. The branching ratio, $\beta_{J'J''}$, corresponding to the emission from the excited level, J′, to level, J″, intermediate between, J′, and the ground state, J, is easily estimated by:

$$\beta_{J'J''} = \frac{A_{J'J''}}{\sum_{J''} A_{J'J''}} \qquad (6)$$

The values of the predicted radiative lifetimes, τ_R, and branching ratio, β, are summarized in Table 4.

Table 4: Calculated branching ratio (β) and lifetime (τ, ms) of prepared glasses.

Transition	Sample 2		Sample 3		Sample 4		Sample 5		Sample 6		Sample 7	
	β	τ in (ms)	β	τ in (ms)	β	τ in (ms)	β	τ in (ms)	β	τ in (ms)	β	τ in (ms)
$^4I_{15/2}\rightarrow{}^4I_{13/2}$	1.0000	1.4176	1.0000	1.2676	1.0000	2.1993	1.0000	1.5521	1.0000	1.5412	1.0000	1.7496
$\rightarrow{}^4I_{11/2}$	0.9277	1.0593	0.9184	1.0078	0.9238	1.7300	0.9274	1.1944	0.9275	1.1745	0.9262	1.3382
$\rightarrow{}^4I_{9/2}$	0.6944	1.0942	0.8400	0.5364	0.6655	1.9796	0.7411	1.0425	0.6981	1.1930	0.6404	1.6255
$^4I_{15/2}\rightarrow{}^4F_{9/2}$	0.9276	0.1183	0.9385	0.0685	0.9249	0.2075	0.9314	0.1182	0.9285	0.1293	0.9243	0.1665
$^4I_{15/2}\rightarrow{}^4S_{3/2}$	0.6968	0.0721	0.6913	0.0685	0.6970	0.1191	0.6953	0.0807	0.6964	0.0793	0.6974	0.0910
$^4I_{15/2}\rightarrow{}^2H_{11/2}$	0.9202	0.0512	0.9100	0.0352	0.9176	0.0833	0.9091	0.0572	0.9118	0.0616	0.9164	0.0728
$^4I_{15/2}\rightarrow{}^4F_{7/2}$	0.8496	0.0373	0.7718	0.0267	0.8582	0.0636	0.8307	0.0394	0.8482	0.0410	0.8666	0.0497

The predicted total spontaneous emission probabilities for the $^4I_{13/2}$ state in the compositions of 75TeO_2-10Nb_2O_5-5PbO-10ZnO-2500 ppm Er_2O_3, 75TeO_2-10Nb_2O_5-5PbO-10ZnO-3750 ppm Er_2O_3, 75TeO_2-10Nb_2O_5-5PbO-10ZnO-5000 ppm Er_2O_3, 75TeO_2-10Nb_2O_5-5PbO-10ZnO-6250 ppm Er_2O_3, 75TeO_2-10Nb_2O_5-5PbO-10ZnO-7500 ppm Er_2O_3 and 75TeO_2-10Nb_2O_5-5PbO-10ZnO-8750 ppm Er_2O_3 glasses are 1.4176, 1.2676, 2.1993, 1.5521, 1.5412 and 1.7496 ms respectively. The present glasses are a good agreement within the range of other laser host glasses doped with Er^{3+} reported in the literature [20- 23]. Hence both the values of the spectroscopic quality factor and the radiative life time of the present glasses are suitable can be used for lasing materials in the infrared range.

The absorption cross-sections of the Er^{3+} ion for the $^4I_{13/2}\rightarrow{}^4I_{15/2}$ transition can be calculated as follows:

$$\sigma_a(\lambda) = \frac{2.303\ .\ OD(\lambda)}{NL} \qquad (7)$$

Where OD (λ) = log (I_0/I) is the optical density of the experimental absorption spectrum, L is the thickness of the sample and N is the concentration of respective rare-earth ions.

The stimulated emission cross-section $\sigma_e(\lambda)$ of Er^{3+} for the $^4I_{13/2} \rightarrow {}^4I_{15/2}$ transition can be deduced from their corresponding ground state absorption cross-section $\sigma_a(\lambda)$ using the follow equation [24]:

$$\sigma_e(\lambda) = \sigma_a(\lambda)\frac{Z_l}{Z_u}\exp\left[\frac{E_{Zl} - hc\lambda^{-1}}{K_B T}\right] \qquad (8)$$

Where Z_l and Z_u are the partition functions for the lower and the upper levels involved in the considered optical transition, T is the room temperature (in this case the room temperature) and E_{ZL} is the zero line energy for the transition between the lower Stark sublevels of the emitting multiplets and the lower Stark sublevels of the receiving multiplets.

Figure 2 shows the calculated absorption and emission cross sections for the prepared glasses doped with Er^{3+} ions. The peak of the stimulated emission cross-section (σ_e^{Peak}) is about 17.75×10^{-21}, 19.13×10^{-21}, 20.91×10^{-21}, 22.50×10^{-21}, 23.98×10^{-21} and 27.96×10^{-21} cm^{-2} for samples 2 to 7 respectively. The highest value of (σ_e^{Peak}) for the emission cross-section is related to the larger value of the line strength of the $^4I_{13/2} \rightarrow {}^4I_{15/2}$. The FWHM of the emission peak is also a critical parameter that is used to evaluate the gain bandwidth properties of the optical amplifiers, it equal 64.53, 66.56, 66, 66, 66.3 and 66.3 nm of sample 2 to7 respectively.

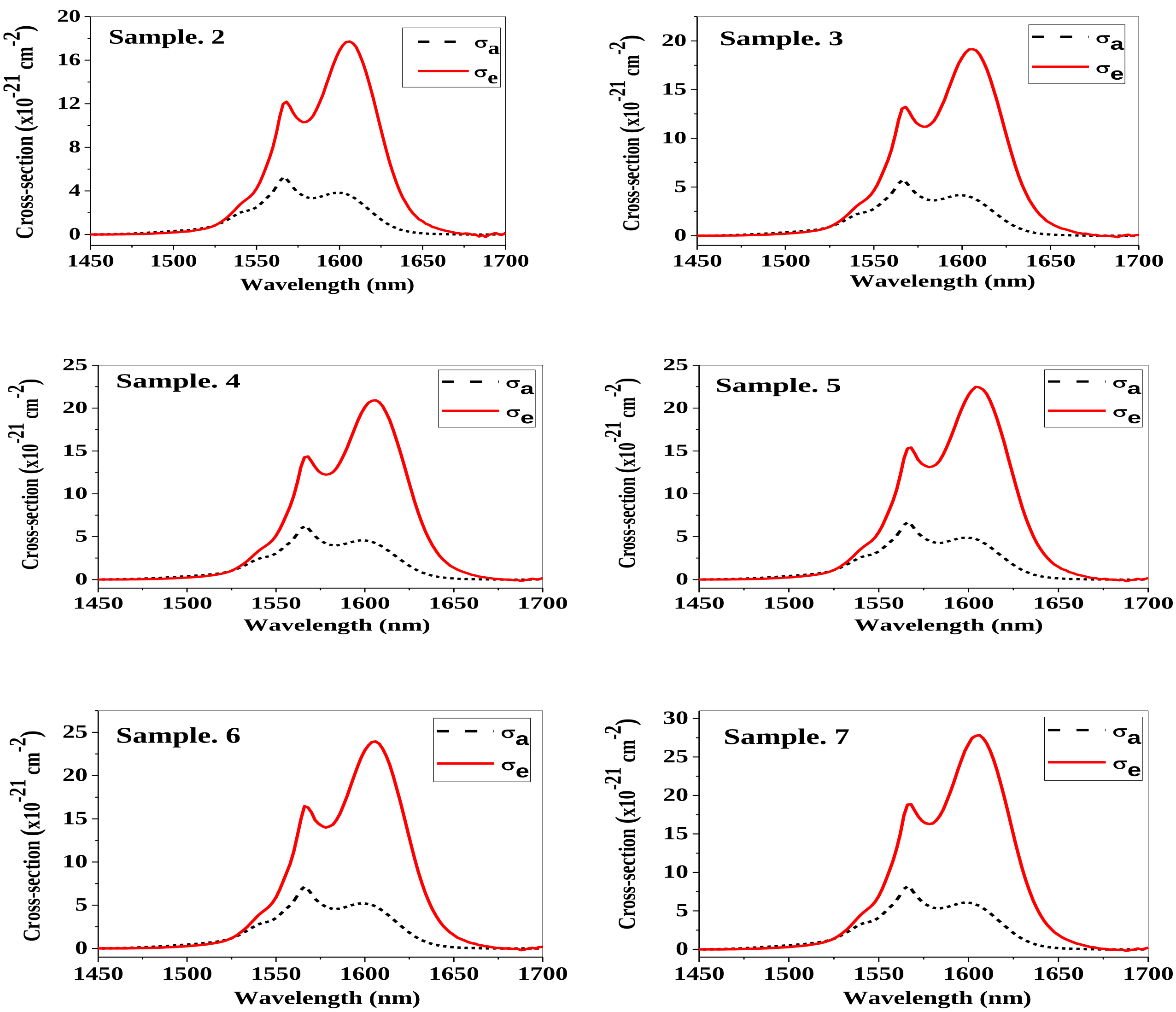

Figure 2: Absorption cross-sections $\sigma_a(\lambda)$ and stimulated emission Cross section $\sigma_e(\lambda)$ of sample 2 to 7.

Due to the large overlap of the absorption and emission spectrum of Er^{3+} ions at 1.5 µm, re-absorption will occur and cause the fluorescence spectrum deformed. Thus, due to the asymmetric profile of the emission line, it is more reasonable to calculate an effective line width, instead of the FWHM. The effective line width (Δλ) can be expressed as $\Delta\lambda = \int \sigma_e(\lambda)d\lambda/\sigma_e^{Peak}$. The effective bandwidths are 65.54, 65.663, 65.65, 65.69, 65.704 and 65.793 nm for sample 2 to 7 respectively. In order to understand the band profile of the $^4I_{13/2} \rightarrow {}^4I_{15/2}$ emission of the Er^{3+} ions and estimate the Stark splitting for the $^4I_{13/2}$ emitting and the $^4I_{15/2}$ ground levels in the studied tellurite glasses, a Gaussian de-convolution of the 1.5 µm band has been performed. Figure 3 shows the emission spectra due to the $^4I_{13/2} \rightarrow {}^4I_{15/2}$ transition of prepared glasses doped with Er^{3+} ions and the deconvolved Gaussian amplitude peaks obtained from the fitting to the emission spectra obtained for Er^{3+}-doped (TNPZ) glass (dotted lines).

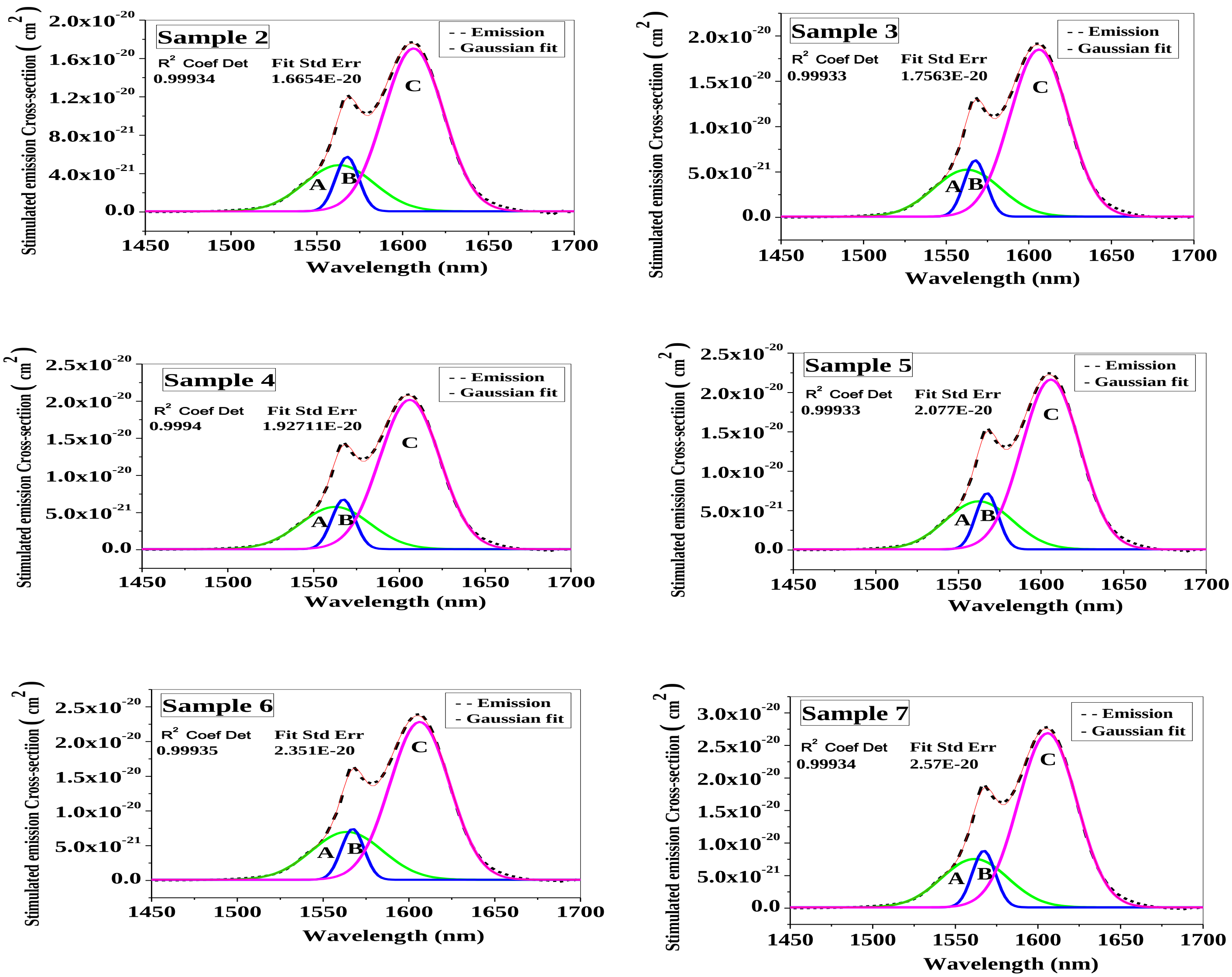

Figure 3: Emission spectra and deconvoluted Gaussian amplitude peaks fitted of sample 2 to 7.

Peak positions and the width of this subcomponent peaks are labeled as A, B and C and tabulated in Table 5. In order to explain the 1.5 µm emission of the Er^{3+} ions, an equivalent model of the four levels system is shown in Fig. 4.The ground $^4I_{15/2}$ level splits into two sublevels at around 0 cm^{-1} and 227 cm^{-1}. The excited $^4I_{13/2}$ level also splits into two sublevels (Starks levels) at around 6570 cm^{-1} and 6700 cm^{-1} together with all of the transitions possible between these subcomponents. The energy differences ΔE_1 = 234–0 = 234 cm^{-1} and ΔE_2= 6394– 6379 = 15 cm^{-1} are corresponding the values of the energy range of the Stark splitting of the $^4I_{15/2}$ and the $^4I_{13/2}$ multiplets, respectively. Also this result also indicates that the bandwidth is strongly dependent on the overall extent of the Stark splitting. The optical gain coefficient is an important factor for evaluating the performance of laser media. The light field intensity derived from the light field power by the simplified relationship$I(Z) = \frac{P(Z)}{A}$, where P(Z) is pump power at the position Z and A is an effective cross sectional area of the core.

Sample of No.	Peak A		Peak B		Peak C	
	λ_A(nm)	W_A(nm)	λ_A(nm)	W_A(nm)	λ_A(nm)	W_A(nm)
Sample2	1563.1	49.6	1567.7	16.982	1606.4	42.8
Sample 3	1562.6	50.28	1567.6	16.31	1606.2	41.44
Sample 4	1562.51	48.24	1567.314	16.32	1606.021	42.124
Sample 5	1562.4	50.3	1567.3	15.63	1606	40.72
Sample 6	1564	48.23	1567.2	15.624	1606.32	41.44
Sample 7	1561.7	48.24	1567.24	16.985	1605.9	42.8

Table 5: Peak positions (λ) and the full widths at the half maximum (W) of the A – C subcomponents.

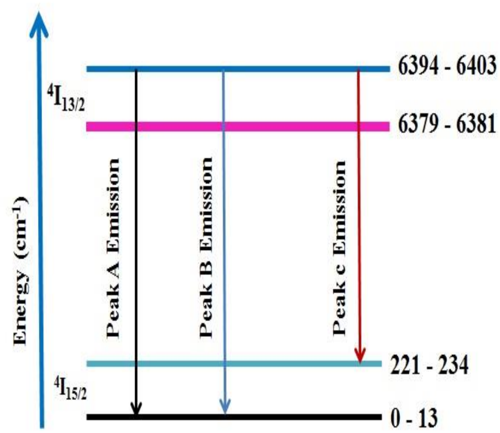

Figure 4: An equivalent model of four level systems for describing 1.5 µm emission of sample 7.

The propagation equation (9) for the pump and signal field power P(Z) in a given direction are thus [25, 26]:

$$\frac{dP(Z)}{dZ} = [\sigma_e N_2(Z) - \sigma_a N_1]P(Z) \qquad (9)$$

Where N is total population volume-density and defined as $N = N_1 + N_2$, N_1 and N_2 represent the population volume-densities of upper and lower levels, respectively. From the absorption and emission cross sections for the transitions between two laser operating levels, the optical gain cross section σ_{gain} that lead to an estimation of the probable operating laser wavelength. If P is the population inversion rate for $^4I_{13/2} \rightarrow {}^4I_{15/2}$ Er^{3+} laser transition, the gain cross section can be calculated using the following relation:

$$\sigma_{gain} = P\,\sigma_{em}(\lambda) - (1 - P)\,\sigma_{abs}(\lambda) \qquad (10)$$

Where σ_{em} and σ_{abs} are emission and absorption cross section, respectively. The wavelength dependence of the gain cross section was calculated for different values of population inversion P (P = 0, 0.1, 0.2,….. , 1) of prepared glasses were shown in Fig. 5. Finally the gain coefficients at 1531 nm of transition $^4I_{13/2} \rightarrow {}^4I_{15/2}$, are 17.70 cm^{-1}, 19.21 cm^{-1}, 20.87 cm^{-1}, 22.50 cm^{-1}, 23.90 cm^{-1}

and 27.80 cm^{-1} for sample 2 to 7, respectively. This value is very large in comparison to those of some tellurite glasses published in the literature [27, 28].

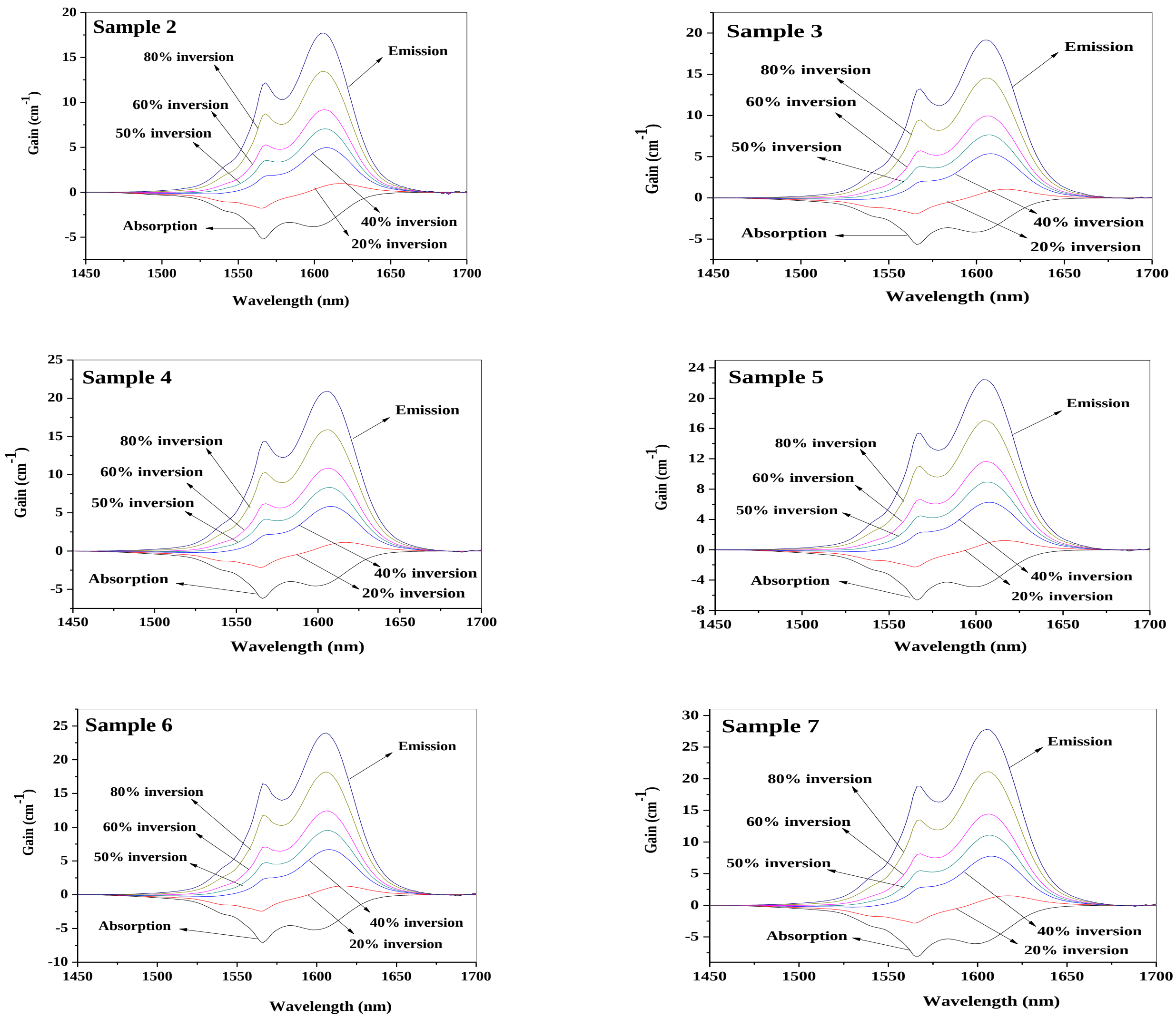

Figure 5: Gain coefficient for $^4I_{13/2} \rightarrow {}^4I_{15/2}$ transitions of sample 2 to 7.

4. Conclusion

The optical properties of the glasses were estimated by measuring UV–Vis-NIR spectroscopy. Studying xEr^{3+} doped $75TeO_2$-$10Nb_2O_5$-5PbO-10ZnO glasses (with x = 0.00, 2500, 3750, 5000, 6250, 7500 and 8750 ppm), shows that the glasses with x = 8750 ppm has the high absorption intensities, emission cross-sections and the JO parameters were used to estimate the radiative probabilities, radiative lifetimes, and branching ratios for different transitions. This shows this glass system especially glasses within composition $75TeO_2$- $10Nb_2O_5$- 5PbO- 10ZnO-8750 ppm Er_2O_3 is suitable as laser material. It has optical gain coefficient of the population inversion of the $^4I_{13/2}$ level (27.80 cm^{-1}) and an effective bandwidth of 66.3 nm.

Acknowledgements

This work was financially supported by the Department of Physics, Faculty of Science, Al- AzharUniv., Cairo Branch, Egypt.

References

[1] Y. Benmadani., A. Kermaoui., M. Chalal., W. Khemici., A. Kellou., F. Pelle., Optical Materials, **35**2234 (2013).
[2] El Sayed Yousef,H. H.Hegazy, Samar Almojadah, M. Reben, Optics &Laser Technology **74**,138 (2015).
[3] M El-Okr, M Ibrahem, M Farouk, Journal of Physics & Chemistry of Solids **69**(10), 2564 (2008).
[4] M Farouk, A Samir, F Metawe, M Elokr, Journal of non-crystalline solids **371**, 14 (2013).
[5] Kamel Damak, El Sayed Yousef, Christian Rüssel, Ramzi. Maâlej, Journal of Quantitative Spectroscopy & Radiative Transfer **134**,55 (2014).
[6] K. Damak, E. Yousef, S. AlFaify, C. Rüssel, R. Maâlej, 1 April 2014/ Vol. 4, No. 4 | Optical Materials Express, **4 (**4),598 (2014).
[7] H. Chen, Y.H. Liu, Y.F. Zhou, Q.Y. Zhang, Z.H. Jiang, J. Non-Cryst. Solids, **351**,3060 (2005).
[8] B. R. Judd, Phys. Rev. **127**, 750 (1961).
[9] G. S. Ofelt, J. Chem. Phys. **37**, 511 (1962).
[10] Y. Ding, S.B. Jiang, B.C. Hang, et al., Opt. Mater.**15**,123 (2000).
[11] R. Lachheb, K. Damak, A.A. Assadi, A. Herrmann, E. Yousef, C. Rüssel, R. Maâlej, Journal of Luminescence, **161**, 281 (2015).
[12] C. Binet, A. Badri, J. C. Lavalley, The Journal of Physical Chemistry,**98** (25),6392 (1994).
[13] L. M. S. El-Deen, M. S. Al Salhi, M. M. Elkholy, Journal of Alloys &Compounds, **465**(1-2),333 (2008).
[14] G. Ghosh, Journal of the American Ceramic Society, **78** (10), 2828 (1995).
[15] Vogel, W., Glass chemistry. Springer-Verlag Berlin. (1994).
[16] H. Lin, S. Tanabe, L. Lin, Y.Y. Hou, K. Liu, D.L. Yang, T.C. Ma, J.Y. Yu, E.Y.B. Pun, J. Lumin.**124**, 167 (2007).
[17] G. Racah, Phys. Rev. **62**, 438 (1942).
[18] W. F. Krupke, IEEE J. Quantum Electron. **10**, 45 (1974).
[19] W.T. Carnall, P.R. Eieids, K. Rajnak, J. Chem. Phys.**49**,4407 (1968).
[20] Y. Ding, S. Jiang, B. Hwang, T. Luo, N. Peyghambarian, Y. Miura, Proc. SPIE 3942 (2000) 166.
[21] H. Ebendorff-Heidepriem, D. Ehrt, M. Bettinelli, A. Speghini, Proc. SPIE 3622 (1999) 19.
[22] M. J. Weber, Phys. Rev. **157**, 262 (1967).
[23] J. Amin, B. Dussardier, T. Schweizer, M. Hempstead, J. Lumin. Vol. **69**, 17 (1996).
[24] X. Zou, H. Toratani, Phys. Rev. B, **52**, 511 (1995).
[25] D. E. McCumber, Phys. Rev. **136**, 954 (1964).
[26] Xujie. Li, Wenjie. Zhang, Phys. B. **403,** 3286 (2008).
[27] Ju H. Choi, Frank G. Shi, Alfred. Margaryan, Ashot. Margaryan, Wytze van der Veer, J. Alloys Comp. **450**,540 (2008).
[28] C. Gheorghe, S. Georgescu, V. Lupei, A. Lupei, and A. Ikesue, J. Appl. Phys. **103,** 083116 (2008).